NJC

Digestive Ripening Yields Atomically Precise Au Nanomolecules.

Journal:	*New Journal of Chemistry*
Manuscript ID	NJ-ART-08-2021-004042.R1
Article Type:	Paper
Date Submitted by the Author:	27-Sep-2021
Complete List of Authors:	Dass, Amala; University of Mississippi, Chemistry and Biochemistry Eswaramoorthy, Senthil Kumar; University of Mississippi, Chemistry and Biochemistry

ARTICLE

Digestive Ripening Yields Atomically Precise Au Nanomolecules.

Senthil Kumar Eswaramoorthy,[a] Amala Dass*,[a]

Received 00th January 20xx,
Accepted 00th January 20xx

DOI: 10.1039/x0xx00000x

Digestive ripening (DR) is a synthetic method where a polydisperse colloid of metal nanoparticles upon refluxing with free ligand in high boiling point solvent gives monodisperse nanoparticles. Brust synthesis is known to form atomically monodisperse thiolate protected gold nanoparticles also known as gold nanomolecules (Au NMs). Unlike Brust method which gives smaller 1-3nm atomically precise nanomole-cules, DR has been used only for the synthesis of large >5nm nanoparticles with good monodispersity. In thiolate protected gold nanoparticle Brust synthesis, the yellow colored phase transferred Au(III) solution is converted to colorless Au(I) mixture after addition of thiol by forming Au-SR, which is then reduced to form black colored Au NMs. Whereas in DR, while using the same primary chemicals, the two steps were reversed: the mixture was reduced before the addition of thiol. Here we show that in DR adding thiol after 2 minutes of reduction gives larger 5 nm particles as reported, whereas adding thiol in 30 seconds after reduction results in smaller < 2 nm particles. In this work for the first time, DR yields atomically precise $Au_{25}(SR)_{18}$ and $Au_{144}(SR)_{60}$ NMs. This is reported using two aliphatic thiols: hexanethiol and dodecanethiol as the protecting ligand. DR was also repeated using an aromatic thiol, 4-tert-butyl benzene thiol (TBBT) which yields $Au_{279}(SR)_{84}$ NMs consistent with the Brust method. Thereby establishing both DR and Brust method leads to the formation of atomic pre-cise Au NMs, regardless of the order of thiol addition and reduction steps.

Introduction

The nanosized metal particles attract huge interest in catalysis, optics, and drug delivery because of its remarkable difference in physical and chemical properties from the respective bulk metals.[1] The nanosized metal particles usage dates back to 4th Century AD, the Lycurgus cup.[2] It has unusual optical effects due to the presence of gold and silver nanoparticles. The size of the particle determines its properties. The catalytic property of noble metals is enhanced when their size is reduced to the nanoscale.[3,4] The size-controlled synthesis of NPs is achieved by manipulating the synthetic conditions. [5,6]

The research of monolayer thiol protected gold nanoparticles (Au NPs) has developed significantly after the introduction of the Brust[7] method. It is a two-phase synthesis (water/toluene) which was later tuned to form atomically monodisperse nanoparticles, also called gold nanomolecules (Au NMs).[8-11] The first major development in the field was hints of monodispersity evidenced by mass spectrometric studies reported by R.L Whetten et al.[11] The next major development, was the crystal structure determination of $Au_{102}(p\text{-}MBA)_{44}$ and $Au_{25}(SCH_2CH_2Ph)_{18}$ proving the atomically monodisperse nature beyond any doubt.[8,9] Later, many other crystal structures have been reported, especially using bulky ligands such as 4-*tert*-butylbenzene thiol (TBBT)[12-14] and tertbutyl thiol.[15-17] Various sizes of NMs protected by different thiolate ligands were obtained by introducing some modifications in the Brust method. But, the basic 3 steps are the same in every Brust method, (i) phase transfer, (ii) addition of thiol, and (iii) reduction using a reducing agent.[7-11,18] In most cases, the basic steps forming the crude mixture involves an etching process to obtain stable sizes. [19]

Ostwald ripening, a diffusion-controlled crystal growth process used for the formation of nanoparticle was proposed in the early to mid-20th Century. In a supersaturated solution, a small change like concentration fluctuation produces a nucleus of a new solid phase which leads to the formation of the nuclei until the degree of supersaturation becomes minimum.[20] Then coalescence occurs in a way that the particles which have a size larger than critical size will gain smaller size particle and grow. The theory of Ostwald ripening was introduced in the work of Lifshitz and Slyozof[21] and further advanced by the work of Wagner,[22] together called as LSW theory.

Digestive ripening (DR) which is also known as inverse Ostwald ripening, involves the etching or dissolution of large NPs into smaller, more stable NPs in the presence of excess capping ligands at a high temperature.[23-25]

DR is one of the commonly used method for synthesizing various sizes of nanoparticles with size monodispersity in different transition metals.[25-27] Various factors affecting the monodispersity and property of the product nanoparticle have been widely studied for this method.[25-31] DR method is also used

[a] *Department of Chemistry and Biochemistry, University of Mississippi, Oxford, MS 38677, United States*

Electronic Supplementary Information (ESI) available: [details of any supplementary information available should be included here]. See DOI: 10.1039/x0xx00000x

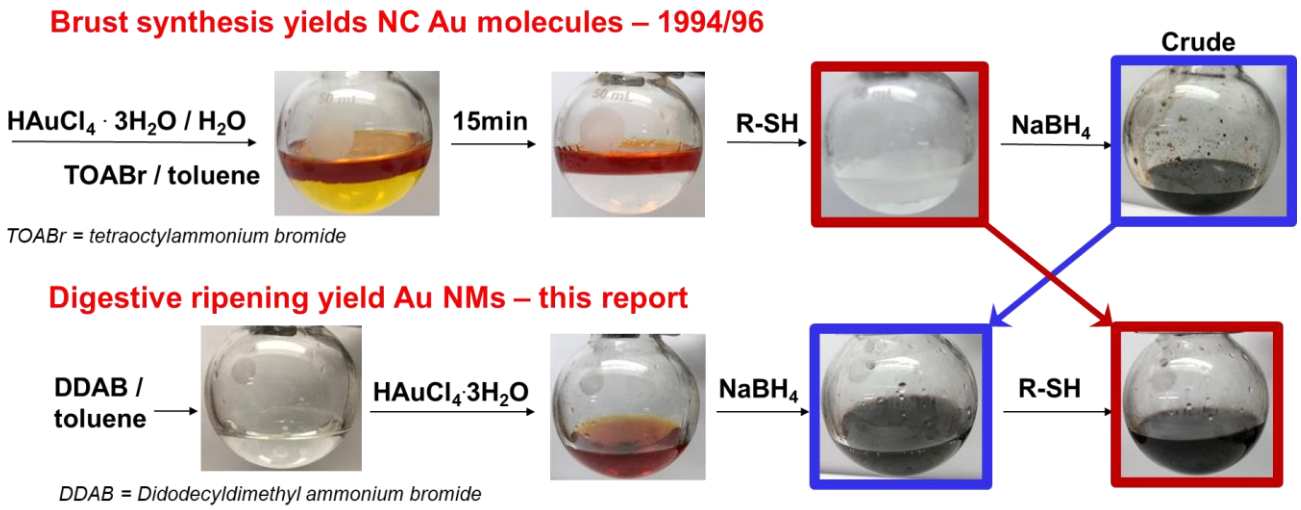

Scheme 1. Synthetic procedure of Brust synthesis method yielding Nanocrystal gold molecules which was reported in 1994[Ref 7] and 1996[Ref 11] directly compared with Digestive ripening yielding gold nanomolecules reported in this work.

to synthesize monolayer thiol protected Au NPs. But the synthesis of atomically monodisperse nanoparticles using the DR method is not yet achieved. In this report we demonstrate in DR using Transmission Electron Microscopy (TEM), adding thiol after 2 minutes of reduction gives larger 5 nm particles as reported, whereas adding thiol in 30 seconds after reduction results in smaller < 2 nm particles. Thereby, we report (i) atomic precision can be achieved in DR by reducing timing (time difference) between reduction of mixture and addition of thiol. (ii) DR yields atomically precise $Au_{25}(SR)_{18}$ and $Au_{144}(SR)_{60}$ NMs. This is reported using two aliphatic thiols: hexanethiol and dodecanethiol as the protecting ligand consistent with reported Au NMs from Brust method.[8, 32, 33] DR was also repeated using an aromatic thiol, TBBT which yields $Au_{279}(SR)_{84}$ NMs.[12] It is consistent with the reported Au NMs from Brust method. Mass spectrometric analysis confirms the atomic precision. (iii) The switching of phase transfer agent to ToABr in DR brings all chemicals (reactant) used for DR and Brust method same, but the steps are different. Especially step two and three mentioned earlier in the Brust method were reversed in DR, but both pathways lead to the formation of atomically precise Au NMs.

Results and Discussion

The step-by-step comparison of the synthetic procedure of Brust and DR method is shown in Scheme 1. The important difference appears at a distinctive step (highlighted by red and blue boxes with arrows), where the reduction of the mixture and addition of thiol steps are reversed. The comparative color change happening in the reactants at each step is evident from the scheme. The Brust method is already known to form atomically precise Au NMs whereas DR is known to form size monodisperse Au NPs (not atomically monodisperse). Here, DR also leads to the formation of atomically precise Au NMs using reported synthetic protocols providing unprecedented results explained below.

Formation of atomic precise small nanoparticles in DR. The DR synthesis was done as mentioned in Scheme 1. Briefly, the Au salt was dissolved in toluene using a phase transfer agent, followed by reduction, and then the addition of capping ligand to the mixture. See the experimental section for more details. Normally in DR after reduction of the mixture the reaction is continued to completion before adding thiol. In Brust method the thiol was already present while reducing the mixture. Here, in DR to obtain smaller gold nanoparticles, we noticed the timing between the reduction of mixture and addition of thiol is crucial. Therefore, addition of thiol was done in two-time differences, soon after the reduction (30 seconds) and after some time (2 minutes). Transmission Electron Microscopy (TEM) image (Figure 1a) of 30 seconds DR product shows particles less than 5 nm in size and its size distribution analysis done by counting the size of 600 particles provides 1.1 ± 0.3 nm (Figure 1C). TEM image of 2-minute DR product (Figure 1b) shows comparatively larger monodisperse spheres and its size distribution based on 400 particles provides 5 ± 0.6 nm (Figure 1d). The particle size drastically dropped from 5nm (Figure 1d) to 1.1 nm when reducing the timing from 2 minutes to 30 seconds. UV-vis spectra of 2 minutes product shown in the inset of Figure 1d has a prominent plasmonic band centered at ~500 nm whereas 30 seconds sample (Figure 1c inset) has a minute feature in the same region. Therefore, this UV-vis spectrum further confirms the drastic drop in size of resulting product by reducing the timing. The addition of capping agent (thiol) soon after reducing the mixture (30 seconds) stops the aggregation of Au into a larger nanoparticle and leads to the formation of particle in Au nanomolecule regime (1 to 2 nm).[34, 35] Further refluxing of the mixture brings all the metastable Au nanoclusters into more stable atomic precise Au NMs.

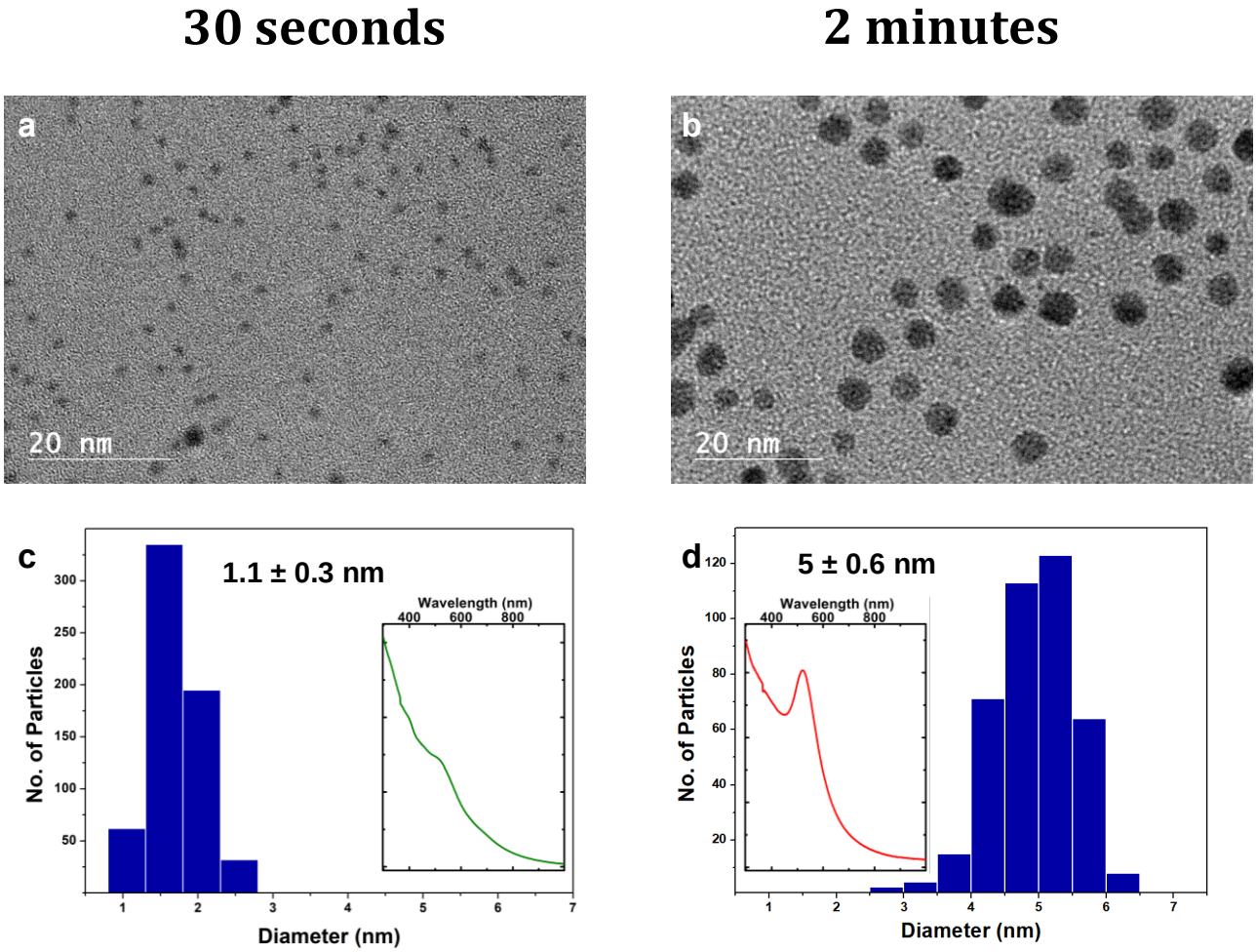

Figure 1. Addition of thiol after 30 seconds of reduction, a) TEM image and c) size distribution plot of its product (UV-vis spectra in the inset). Addition of thiol after 2 minutes of reduction b) TEM image and d) size distribution plot of its product (UV-vis spectra in the inset).

DR yields Au NMs with aliphatic thiols. The DR product was then analyzed in Matrix Assisted Laser Desorption Time of Flight (MALDI-MS) mass spectrometry using the DCTB matrix.[33] The low and high laser intensity MALDI-MS data exhibits various sizes in the product. In high laser intensity, the nanoclusters tend to fragment, but higher laser fluence is needed to ionize all the sizes present in the product. The high laser data of hexanethiol protected Au NMs product in Figure 2a shows the presence of two products, namely at 7 and 30 kDa. The exact mass with high accuracy can be determined Electrospray Ionization Mass Spectrometry (ESI-MS). The ESI-MS spectrum in Figure 2b predominantly shows 3 sizes of nanoclusters namely $Au_{25}(SR)_{18}$, $Au_{137}(SR)_{56}$, and $Au_{144}(SR)_{60}$. In Figure 2b, 17,698 Da and 11,799 Da peaks are observed, representing 2+ and 3+ charge peaks of $Au_{144}(SR)_{60}$ which has a molecular weight of 35,397 Da. Similarly, 2+ and 3+ charge state of $Au_{137}(SR)_{56}$ peaks are observed at 16,774 Da and 11,183 Da. The 1+ charge state of $Au_{25}(SR)_{18}$, 7,034 Da is also observed in Figure 2b. The same synthesis protocol is repeated in another aliphatic thiol, dodecanethiol. The same 3 sizes are observed in dodecanethiol as shown in Figure S1. Figure S1a shows the MALDI-MS spectra of dodecanethiol protected nanoclusters synthesized using the DR method. The high laser data reveals the formation of 2 sizes, one around 7 kDa and a broad peak at 32 kDa. The low laser data on Figure S1a shows the peak of $Au_{25}(SR)_{18}$, the adjacent peak is characteristic MALDI fragmentation of $Au_4(SR)_4$. ESI-MS data on Figure S1b showing a 1+ charge state of $Au_{25}(SR)_{18}$ confirms the same. The broad peak in 32 kDa of MALDI-MS has 2 species which is confirmed by its respective ESI-MS spectra in Figure S1b. The 2 species are $Au_{144}(SR)_{60}$ (3+ and 4+ charge state peaks marked in Figure S1b) and $Au_{137}(SR)_{56}$ (3+ charge state peak marked in Figure S1b). From the extensive research in thiolate protected nanoclusters, the linear chain aliphatic thiol makes a unique series ($Au_{25}(SR)_{18}$, $Au_{38}(SR)_{24}$, $Au_{137}(SR)_{56}$, $Au_{144}(SR)_{60}$) from the Brust method of synthesis.[34-36] The same series containing $Au_{25}(SR)_{18}$, $Au_{137}(SR)_{56}$ and $Au_{144}(SR)_{60}$ is observed in this work using the DR method.

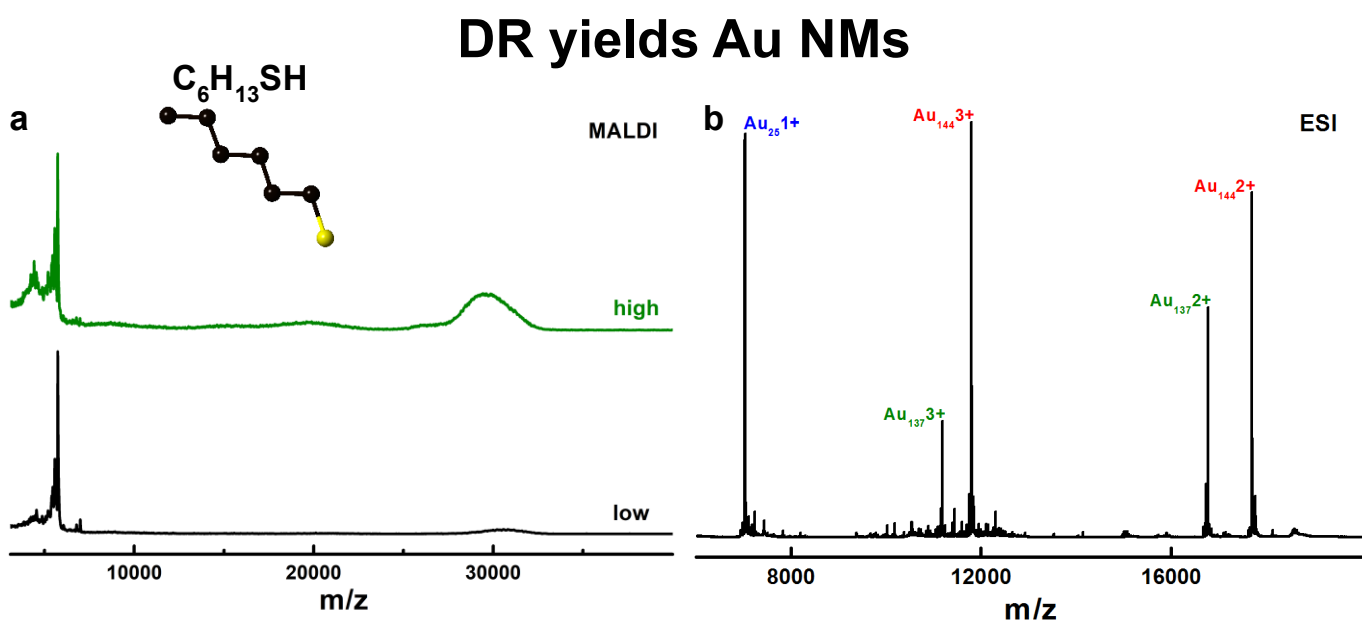

Figure 2. Mass spectrum of the digestive ripening synthesis product showing atomically precise nanomolecules protected by hexanethiol. (a) MALDI-MS data of digestive ripening synthesis product showing high (green) and low (black) laser. (b) ESI-MS data of the same product showing the presence of $Au_{144}(SR)_{60}$, $Au_{137}(SR)_{54}$ and $Au_{25}(SR)_{18}$ species.

Figure S2 shows the optical property of the Au NMs protected by hexanethiol and dodecanethiol. The $Au_{144}(SR)_{60}$ and $Au_{137}(SR)_{54}$ do not have prominent optical features in the UV-vis region.[32, 37] But as in Figure S2, both spectra exhibit a small plasmonic resonance feature at ~500 nm. It indicates the presence of larger species in the plasmonic range in small amount.

DR yields Au NMs using aromatic thiol (TBBT). The same synthesis protocol was followed with a different thiol, 4-*tert*-butylbenzenethiol (TBBT). Unlike aliphatic thiols, in TBBT the sulfur atom is attached to the phenyl ring. Additionally, it has a tertiary group attached to the para position of the phenyl ring. This gives different electronic, steric, and π-π ligand interaction properties to the product Au NMs.[38] As a result, it gives a whole different series of Au NMs.[38, 39] This series is called aromatic series as the sulfur is directly attached to the phenyl ring.[38] Figure 3a is the MALDI-MS spectrum data of TBBT protected Au NMs. It shows a peak at ~62 kDa in low laser intensity (black) corresponding to $Au_{279}(SR)_{84}$ species as reported using Brust method of synthesis.[12] High laser intensity shows the same species, but only gold core mass ~55 kDa. This is because of the removal of surface ligands in presence of higher laser intensity. ESI-MS spectrum in Figure 3b shows 3+ (22,945 Da), 4+ (17,209 Da) and 5+ (13,767 Da) of $Au_{279}(SR)_{84}$ species.

Isolation of pure Au NMS using Size Exclusion Chromatography (SEC). DR gives a mixture of Au NMs sizes as discussed earlier. SEC is one of the best methods used for isolation of Au NMs based on the size.[40, 41] Here, SEC is used to isolate pure Au NMs from final DR product containing mixture of sizes. The size separated and purified DR samples can then be compared with previously reported Brust method using similar purification techniques.[8, 9, 12, 15-17, 32, 33, 37, 42] Figure S3b and S4b shows the SEC column during the last stage of separation. Both images (Figure S3b and S4b) have two nicely separated bands, first at the bottom, a black band with 30 kDa species having majorly $Au_{144}(SR)_{60}$ and a second, reddish brown band on the top is pure $Au_{25}(SR)_{18}$. SEC isolated MALDI-MS data of hexane thiol protected Au NMs shown in Figure S5a, and corresponding ESI-MS data shown in Figure S5b, top red spectra showing only 30 kDa peak in MALDI and 3+ peak of $Au_{144}(SR)_{60}$ and $Au_{137}(SR)_{54}$ confirms the isolation of 30 kDa species. Similarly, bottom black spectra showing $Au_{25}(SR)_{18}$ peak in MALDI-MS data and 1+ peak of $Au_{25}(SR)_{18}$ in ESI-MS data confirms the isolation of $Au_{25}(SR)_{18}$. UV-vis spectrum of (Figure S3a, red) the isolated $Au_{144}(SR)_{60}$ exhibits no distinctly observed peaks but minor peaks at ~510 nm and ~700 nm. It is consistent withthe previously reported works and confirms the purity.[32, 42] Similarly, UV-vis spectrum of $Au_{25}(SR)_{18}$ (Figure S3a, black) showing well defined peaks at 400, 450, and 670nm and slight shoulder peaks at ~575 and ~815 nm as previously reported.[35, 36, 43]

Likewise, Figure S6 exhibits the isolation of 30 kDa and 8 kDa of dodecanethiol protected Au NMs using MALDI-MS and ESI-MS. Figure S4a confirms the purity of isolation through UV-vis spectra.[32, 36, 42] These results using two different ligands (hexane thiol and dodecanethiol) confirm that DR synthesis produces atomically monodisperse nanomolecules that match with previously reported Brust synthesis.[32, 36, 42]

Mass Spectrometry comparison of DR and Brust methods. Samples were prepared using the 2-phase Brust method for comparison purposes. The dodecanethiol protected NMs are synthesized using the Brust method as mentioned in the experiment section. The MALDI mass spectrum comparison of

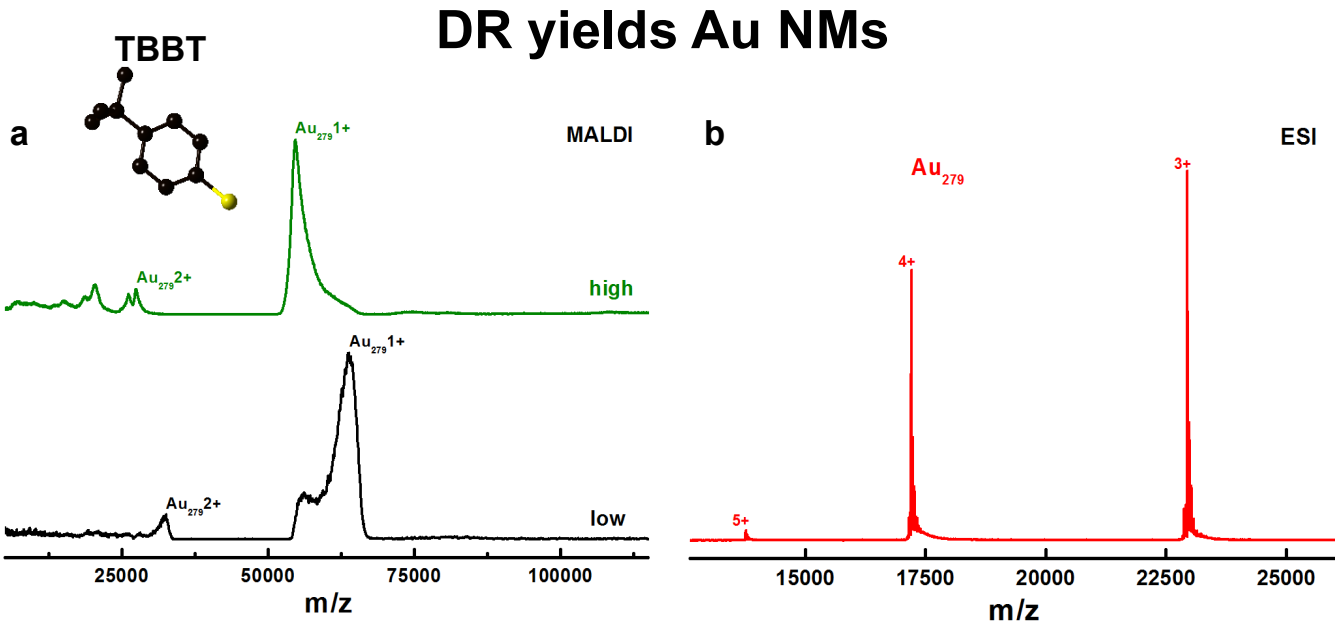

Figure 3. Mass spectrum confirming the repeatability of the digestive ripening yielding atomically precise gold nanomolecules with rigid secondary ligand (TBBT) where S is directly attached to phenyl ring. (a) High (green) and low (black) laser intensity MALDI-MS of the digestive ripened product. (b) ESI-MS of the digestive ripened product showing 3+, 4+ and 5+ of $Au_{279}(SR)_{84}$.

DR and Brust syntheses, as in Figure S7, shows that they both have 2 distinct peaks at 7 and 32 kDa. Their corresponding ESI-MS data comparison shown in Figure 4, depicts the 3+ charge state of $Au_{144}(SR)_{60}$ (13,482 Da) and $Au_{137}(SR)_{54}$ (12,754 Da). Figure 4 also shows 1+ charge state of $Au_{25}(SR)_{18}$ (8,549 Da) in both methods. This confirms that final product in both methods have three Au NMs, namely $Au_{144}(SR)_{60}$, $Au_{137}(SR)_{54}$ and $Au_{25}(SR)_{18}$. Therefore, these results suggest that *DR and Brust lead to the same product despite their pathway*. The SEC purified DR synthesis product shown in Figure S3 to S6 is consistent with reported works using Brust method.[32, 38] Different conditions (temperature, time, etc.) and molar ratios are used to synthesize various sizes of the same thiolate protected Au NMs in Brust synthesis method.[34, 44] This forms a unique series of specified number of gold and thiolate protected Au NMs. The DR synthesis method used in this report also gave 3 sizes, which is a part of the unique series.[38] The recent publication of $Au_{\sim 2000}(SR)_{\sim 290}$ provided the largest highly stable unique nanocluster using the Brust method as ~3.8 nm[44] which is smaller compared to normal sizes reported in the DR method.[23, 25-27]

The step-by-step comparison of the synthetic procedure of Brust and DR method shown in Scheme 1. The important difference between the two methods is highlighted (red and blue box with arrows). Scheme 1 highlights the change in the color of the products inside each reaction flask.

The formation of these nanoclusters is based on a hypothesis from the Brust method,[7, 10, 45, 46] which was developed based on the color change at every step. Similar Brust-like synthesis in the formation of thiolate protected Ag nanocrystals is also reported.[47] In the reported hypothesis, ToABr was used as a phase transfer agent to transfer the Au^{3+} gold salt to organic phase. Here the color is reddish orange (2nd image in top of Scheme 1) representing 3+ charge state, Au^{3+}. Then the introduction of thiol reduces the 3+ charge state to 1+ forming an $Au_n(SR)_m$ complex, representing the gradual color change from reddish orange to colorless (3rd image in top of Scheme 1). Followed by reduction using sodium borohydride produced stable nanoparticles, with a Au(0) core, as indicated by the black color (Scheme 1 rightmost image on top), with a neutral charge state in the core Au atoms. The thermochemical treatment of this obtained crude product converts all the meta-stable products into highly stable ones. As mentioned in Scheme 1, the major change in DR from Brust is inter-changed steps between the reduction of the mixture (blue highlighted) and the addition of thiol (red highlighted). Experimental data backed up by above mass spectrometry results shows that regardless of the change in thiol addition and borohydride reduction steps, both DR and Brust synthesis give the same products. However, the DR procedure contradicts the above mentioned hypothesis as there is no involvement of thiol at the reduction step whereas the hypothesis involves formation of $Au_n(SR)_m$ polymer before reduction.

On the other hand, Tong and coworkers reported mechanistic studies on the Brust method, where they argue that even though thiol was added before reduction, Au-S bond is not formed until the reduction step. They also argue that instead of formation of $Au_n(SR)_m$ complex, Au forms a complex with ToABr.[48-52] Meanwhile, some one-phase Brust synthesis does not include phase transfer agent in its synthesis process which

could not be explained by Tong and coworkers mechanistic study.[53, 54]

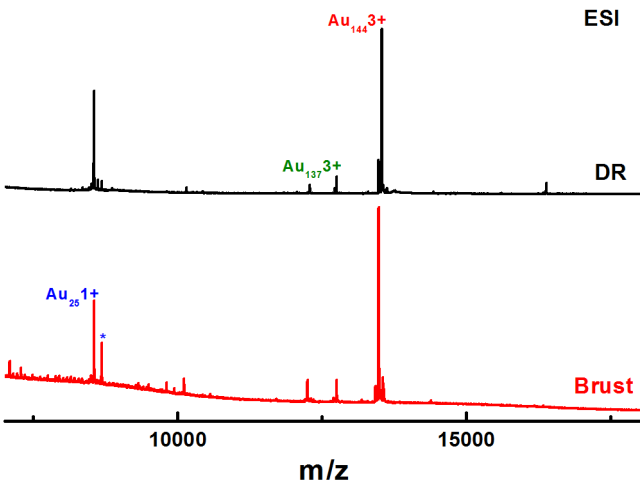

Figure 4. ESI Mass spectrum comparison of dodecanethiol protected atomically precise nanoparticle synthesized using Digestive Ripening (top) and Brust (bottom) method. (* is Cs^+ adduct.)

Difference between 2 methods. As mentioned earlier, synthesis of nanoclusters using the Brust method was highly monodisperse as confirmed by mass spectrometry and single-crystal XRD, also by their optical properties.[55, 56] Whereas the DR is used only for synthesizing nanoparticles which are not atomically monodisperse (only size monodisperse).[26, 28, 29] However, the above results from three different thiols confirm that through DR, atomically precision is achievable. A keen observation suggests that the precursors used in both methods are the same with one difference, DR uses Didodecyldimethylammonium bromide (DDAB) as a phase transfer agent whereas the Brust method uses Tetra octyl Ammonium Bromide (ToABr). The crude product was etched at 80 °C in Brust synthesis, but in DR the product was refluxed. Temperature is known to affect the formation of Au NMs.[57] Here, the Brust synthesis and DR are optimized to obtain the reported Au NMS. A prolonged refluxing results in decomposition of products.[57]

To eliminate the influence of the phase transfer agent, the DR method is repeated the same with a change of phase transfer agent to ToABr. The results are shown in Figure S9 using hexanethiol protected Au NMs. The MALDI spectrum in Figure S9a reveals the presence of a broad peak around 30 kDa with a small peak around 7 kDa and some high mass peaks, similar to the same hexanethiol protected Au NMs synthesized using DDAB shown in Figure 2a. The 30 kDa peaks exactly match with the MALDI spectrum in Figure 1a explaining the presence of $Au_{137}(SR)_{54}$ and $Au_{144}(SR)_{60}$ species, also 7 kDa species corresponding to $Au_{25}(SR)_{18}$ similar to Figure 2a. These $Au_{144}(SR)_{60}$ and $Au_{137}(SR)_{54}$ species are confirmed by ESI-MS spectra in Figure S9b, where 2+ and 3+ of both $Au_{144}(SR)_{60}$ and $Au_{137}(SR)_{54}$ were observed. These observations proved that the change in the phase transfer agent in DR has no impact on the formation of the Au NMs. ToABr affects a little in the relative amounts of the various sizes of Au NMs, but eventually, it leads to the formation of same Au NMs. Therefore, by keeping all chemicals same, both DR and Brust synthesis give the same products, regardless of the change in thiol addition and borohydride reduction steps.

Conclusions

In conclusion, this study reveals that digestive ripening can yield atomically precise Au NMs. The atomic precision is achieved by reducing the time difference between reduction of the mixture and addition of thiol. The consistency of this process was confirmed using three different thiols. Two aliphatic thiols give $Au_{25}(SR)_{18}$, $Au_{137}(SR)_{54}$, and $Au_{144}(SR)_{60}$, a series of Au NMs with a distinct number of gold and thiolate ligands. Structurally rigid third ligand TBBT, where sulfur atom is directly attached to the phenyl ring, gives $Au_{279}(SR)_{84}$, an entirely different series of Au NMs. The comparison of the digestive ripening results with the Brust method infers that despite major changes in the procedure, both methods lead to the formation of Au NMs. The aliphatic and aromatic series of Au NMs identified in the Brust method is also seen in the DR method. These new findings opened a new path from the long-believed mechanism of the Brust method. Then paved a way for future work on a study of the underlying mechanism for the formation of Au NMs, which should satisfy both pathways. The DR result using ToABr eliminates the influence of any difference in the chemicals and reiterates that Brust and DR yield the same Au NMs despite the difference in their pathways.

Experimental

Materials

Hydrogen tetrachloroaurate(III) trihydrate ($HAuCl_4.3H2O$) (Alfa aesar, 99.99%), Tetraoctylammonium bromide (ToABr) (Aldrich, 98%), Didodecyldimethylammonium bromide (DDAB)(Acros, 99%), Sodium borohydride (NaBH4, 99%), 4-tert-butylbenzenethiol (TBBT)(TCI, 99%), 1-Dodecanethiol (Acros, 98%), 1-Hexanethiol (Aldrich), Cesium acetate (Acros, 99%), and trans-2-[3[(4-tertbutyl-phenyl)-2-methyl-2 propenylidene]malononitrile (DCTB matrix) (Fluka ≥ 99%). HPLC grade solvents such as tetrahydrofuran, toluene, and methanol were obtained from Fisher Scientific. All the materials were used as received.

Synthesis:

The synthesis was done based on previous report.[26] The synthesis method comprises 2 parts. First, The Didodecyldimethylammonium bromide (DDAB) (110 mg) was dissolved in toluene. Then $HAuCl_4.3H_2O$ (40 mg) was added to the above solution and transferred to Round Bottom Flask (RBF). Typically, $HAuCl_4.3H_2O$ does not dissolve in Toluene, but using DDAB as a phase transfer agent, it can be dissolved in toluene. The solution was stirred for 15

minutes to get thorough mixing. The mixture was then reduced by $NaBH_4$(18 mg) in water, which indicated by the solution turning black. After 30 seconds, hexanethiol (0.43 mL) (Au:thiol = 1:30) was added rapidly, and the solution was stirred for 1 hour. The same thiol ratio maintained in reaction with other two thiols. Second, the RBF was connected to a refluxing condenser and refluxed for 18 hours. Finally, the refluxing was stopped, and the temperature was allowed to reach room temperature. The solution was rotary evaporated to remove the excess solvent. The resulted product was washed with methanol and water mixture (3-4 times) to remove excess thiol and by-products. The same method was repeated by only changing the phase transfer agent as ToABr for comparison with the Brust method.

The Brust synthesis was carried by small changes in Brust[7] two-phase synthesis. First, ToABr (0.14 g) was dissolved in toluene (7.5 ml) in an RBF. Then $HAuCl_4.3H_2O$ (0.1 g) was dissolved in distilled water (10 ml) added to the toluene solution. The mixture was stirred for 30 minutes. The colour of the organic phase changed to bright orange, indicating phase transfer was complete. Water was discarded. The whole setup was transferred to an ice bath and stirring continued for 30 minutes. 120 μL of 1-Dodecanethiol (Au:thiol= 1:2) was added and stirring continued for 30 minutes. The solution turned white. The mixture was reduced by $NaBH_4$ (0.1 mg) in 5 ml ice-cold water, immediately the colour changed to black. The solution was further stirred for 3 hours. Then the solvent was removed from the product and washed with the water-methanol mixture about 3 times, and the resulting crude was separated. The crude product was redistributed in toluene (1 mL) with an excess amount of 1-dodecanethiol and etched at 80 °C for 2 days. The resulting product was washed with the water-methanol mixture, and the final product was obtained.

Conflicts of interest

There are no conflicts to declare.

Acknowledgements

NSF-CHE-1808138 supported the performed work. We acknowledge Rooban Venkatesh K G Thirumala for his assistance with TEM image collection.

Notes and references

1. A. C. Templeton, W. P. Wuelfing and R. W. Murray, *Acc. Chem. Res.*, 2000, **33**, 27-36.
2. D. J. Barber and I. C. Freestone, *Archaeometry*, 1990, **32**, 33-45.
3. E. L. Downs and D. R. Tyler, *Coord. Chem. Rev.*, 2014, **280**, 28-37.
4. J. Fang, B. Zhang, Q. Yao, Y. Yang, J. Xie and N. Yan, *Coord. Chem. Rev.*, 2016, **322**, 1-29.
5. S. Sun, P. Mendes, K. Critchley, S. Diegoli, M. Hanwell, S. D. Evans, G. J. Leggett, J. A. Preece and T. H. Richardson, *Nano Lett.*, 2006, **6**, 345-350.
6. P. A. Schaal, A. Besmehn, E. Maynicke, M. Noyong, B. Beschoten and U. Simon, *Langmuir*, 2012, **28**, 2448-2454.
7. M. Brust, M. Walker, D. Bethell, D. J. Schiffrin and R. Whyman, *J. Chem. Soc., Chem. Commun.*, 1994, 801-802.
8. M. W. Heaven, A. Dass, P. S. White, K. M. Holt and R. W. Murray, *J. Am. Chem. Soc.*, 2008, **130**, 3754-3755.
9. P. D. Jadzinsky, G. Calero, C. J. Ackerson, D. A. Bushnell and R. D. Kornberg, *Science*, 2007, **318**, 430-433.
10. T. G. Schaaff and R. L. Whetten, *J. Phys. Chem. B*, 1999, **103**, 9394-9396.
11. R. L. Whetten, J. T. Khoury, M. M. Alvarez, S. Murthy, I. Vezmar, Z. L. Wang, P. W. Stephens, C. L. Cleveland, W. D. Luedtke and U. Landman, *Adv. Mater.*, 1996, **8**, 428-433.
12. N. A. Sakthivel, S. Theivendran, V. Ganeshraj, A. G. Oliver and A. Dass, *J. Am. Chem. Soc.*, 2017, **139**, 15450-15459.
13. C. Zeng, Y. Chen, K. Kirschbaum, K. Appavoo, M. Y. Sfeir and R. Jin, *Sci. Adv.*, 2015, **1**, e1500045.
14. C. Zeng, H. Qian, T. Li, G. Li, N. L. Rosi, B. Yoon, R. N. Barnett, R. L. Whetten, U. Landman and R. Jin, *Angew. Chem. Int. Ed.*, 2012, **51**, 13114-13118.
15. D. Crasto and A. Dass, *J. Phys. Chem. C*, 2013, **117**, 22094-22097.
16. D. Crasto, S. Malola, G. Brosofsky, A. Dass and H. Häkkinen, *J. Am. Chem. Soc.*, 2014, **136**, 5000-5005.
17. H. Yang, Y. Wang, A. J. Edwards, J. Yan and N. Zheng, *Chem. Commun.*, 2014, **50**, 14325-14327.
18. S. G. Booth, A. Uehara, S. Y. Chang, C. La Fontaine, T. Fujii, Y. Okamoto, T. Imai, S. L. M. Schroeder and R. A. W. Dryfe, *Chem. Sci.*, 2017, **8**, 7954-7962.
19. Y. Cao, T. Liu, T. Chen, B. Zhang, D.-e. Jiang and J. Xie, *Nature Communications*, 2021, **12**, 3212.
20. A. Bhakta and E. Ruckenstein, *J. Chem. Phys*, 1995, **103**, 7120-7135.
21. I. M. Lifshitz and V. V. Slyozov, *J. Phys. Chem. Solids*, 1961, **19**, 35-50.
22. C. Wagner, *Zeitschrift für Elektrochemie, Berichte der Bunsengesellschaft für physikalische Chemie*, 1961, **65**, 581-591.
23. X. Lin, Sorensen, C. & Klabunde, K., *J. Nanopart. Res.*, 2000, **2**, 157-164.
24. D. Jose and B. R. Jagirdar, *J. Phys. Chem. C*, 2008, **112**, 10089-10094.
25. J. R. Shimpi, D. S. Sidhaye and B. L. V. Prasad, *Langmuir*, 2017, **33**, 9491-9507.
26. J. Seth and B. L. V. Prasad, *Nano Research*, 2016, **9**, 2007-2017.
27. P. Sahu and B. L. V. Prasad, *Nanoscale*, 2013, **5**, 1768-1771.
28. B. L. V. Prasad, S. I. Stoeva, C. M. Sorensen and K. J. Klabunde, *Langmuir*, 2002, **18**, 7515-7520.
29. M.-L. Lin, F. Yang and S. Lee, *Colloids Surf.*, 2014, **448**, 16-22.
30. P. Sahu and B. L. V. Prasad, *Chem. Phys. Lett.*, 2012, **525-526**, 101-104.
31. P. Wang, X. Qi, X. Zhang, T. Wang, Y. Li, K. Zhang, S. Zhao, J. Zhou and Y. Fu, *Nanoscale Res. Lett.*, 2017, **12**, 25.
32. H. Qian and R. Jin, *Chem. Mater.*, 2011, **23**, 2209-2217.
33. A. Dass, A. Stevenson, G. R. Dubay, J. B. Tracy and R. W. Murray, *J. Am. Chem. Soc.*, 2008, **130**, 5940-5946.
34. C. Kumara, X. Zuo, J. Ilavsky, K. W. Chapman, D. A. Cullen and A. Dass, *J. Am. Chem. Soc.*, 2014, **136**, 7410-7417.
35. M. Zhu, E. Lanni, N. Garg, M. E. Bier and R. Jin, *J. Am. Chem. Soc.*, 2008, **130**, 1138-1139.
36. Z. Luo, V. Nachammai, B. Zhang, N. Yan, D. T. Leong, D.-e. Jiang and J. Xie, *J. Am. Chem. Soc.*, 2014, **136**, 10577-10580.
37. V. R. Jupally, A. C. Dharmaratne, D. Crasto, A. J. Huckaba, C. Kumara, P. R. Nimmala, N. Kothalawala, J. H. Delcamp and A. Dass, *Chem. Commun.*, 2014, **50**, 9895-9898.

38. M. Rambukwella, N. A. Sakthivel, J. H. Delcamp, L. Sementa, A. Fortunelli and A. Dass, *Front. Chem.*, 2018, **6**.
39. N. A. Sakthivel and A. Dass, *Acc. Chem. Res.*, 2018, **51**, 1774-1783.
40. S. Knoppe, J. Boudon, I. Dolamic, A. Dass and T. Bürgi, *Anal. Chem.*, 2011, **83**, 5056-5061.
41. N. A. Sakthivel, V. R. Jupally, S. K. Eswaramoorthy, K. H. Wijesinghe, P. R. Nimmala, C. Kumara, M. Rambukwella, T. Jones and A. Dass, *Anal. Chem.*, 2021, **93**, 3987-3996.
42. N. K. Chaki, Y. Negishi, H. Tsunoyama, Y. Shichibu and T. Tsukuda, *J. Am. Chem. Soc.*, 2008, **130**, 8608-8610.
43. Y. Shichibu, Y. Negishi, T. Tsukuda and T. Teranishi, *J. Am. Chem. Soc.*, 2005, **127**, 13464-13465.
44. S. Vergara, U. Santiago, C. Kumara, D. Alducin, R. L. Whetten, M. Jose Yacaman, A. Dass and A. Ponce, *J. Phys. Chem. C*, 2018, **122**, 26733-26738.
45. S. Chen, A. C. Templeton and R. W. Murray, *Langmuir*, 2000, **16**, 3543-3548.
46. Y.-S. Shon, C. Mazzitelli and R. W. Murray, *Langmuir*, 2001, **17**, 7735-7741.
47. J. García-Barrasa, J. M. López-de-Luzuriaga, M. Monge, K. Soulantica and G. Viau, *J. Nanopart. Res.*, 2011, **13**, 791-801.
48. Y. Li, O. Zaluzhna and Y. J. Tong, *Langmuir*, 2011, **27**, 7366-7370.
49. Y. Li, O. Zaluzhna, B. Xu, Y. Gao, J. M. Modest and Y. J. Tong, *J. Am. Chem. Soc.*, 2011, **133**, 2092-2095.
50. O. Zaluzhna, Y. Li, T. C. Allison and Y. J. Tong, *J. Am. Chem. Soc.*, 2012, **134**, 17991-17996.
51. O. Zaluzhna, Y. Li, C. Zangmeister, T. C. Allison and Y. J. Tong, *Chem. Commun.*, 2012, **48**, 362-364.
52. P. J. G. Goulet and R. B. Lennox, *J. Am. Chem. Soc.*, 2010, **132**, 9582-9584.
53. A. Dass, T. Jones, M. Rambukwella, D. Crasto, K. J. Gagnon, L. Sementa, M. De Vetta, O. Baseggio, E. Aprà, M. Stener and A. Fortunelli, *J. Phys. Chem. C*, 2016, **120**, 6256-6261.
54. T. C. Jones, L. Sumner, G. Ramakrishna, M. b. Hatshan, A. Abuhagr, S. Chakraborty and A. Dass, *J. Phys. Chem. C*, 2018, **122**, 17726-17737.
55. M. S. Devadas, J. Kim, E. Sinn, D. Lee, T. Goodson and G. Ramakrishna, *J. Phys. Chem. C*, 2010, **114**, 22417-22423.
56. S. Knoppe and T. Bürgi, *Acc. Chem. Res.*, 2014, **47**, 1318-1326.
57. T. Chen, Q. Yao, X. Yuan, R. R. Nasaruddin and J. Xie, *J. Phys. Chem. C*, 2017, **121**, 10743-10751.